



Published in final edited form as:

Am J Surg Pathol. 2016 August ; 40(8): 1009–1020. doi:10.1097/PAS.0000000000000629.

Recurrent *BCOR* Internal Tandem Duplication and *YWHAE-NUTM2B* Fusions in Soft Tissue Undifferentiated Round Cell Sarcoma of Infancy – Overlapping Genetic Features with Clear Cell Sarcoma of Kidney

Yu-Chien Kao, MD^{1,2}, Yun-Shao Sung, MSc², Lei Zhang, MD², Shih-Chiang Huang, MD^{2,3}, Pedram Argani, MD⁴, Catherine T Chung, MD⁵, Nicole S. Graf, FRCPA⁶, Dale C. Wright, FHGSA, ARCPA⁷, Stewart J. Kellie, FRACP, MD⁸, Narasimhan P Agaram, MD², Kathrin Ludwig, MD⁹, Angelica Zin, PhD⁹, Rita Alaggio, MD¹⁰, and Cristina R. Antonescu, MD²

¹Department of Pathology, Shuang Ho Hospital, Taipei Medical University, Taipei, Taiwan

²Department of Pathology, Memorial Sloan Kettering Cancer Center, New York, NY, USA

³Department of Anatomical Pathology, Chang Gung Memorial Hospital, Chang Gung University College of Medicine, Taoyuan, Taiwan

⁴Departments of Pathology and Oncology, Johns Hopkins University School of Medicine, Baltimore, Maryland, USA

⁵Division of Pathology, Department of Paediatric Laboratory Medicine, The Hospital for Sick Children, Toronto, Ontario, Canada

⁶Department of Histopathology, University of Sidney, The Children's Hospital at Westmead, Sydney, New South Wales, Australia

⁷Department of Cytogenetics, Sydney Genome Diagnostics, Sydney, New South Wales, Australia

⁸Pediatric Oncology Department, University of Sidney, The Children's Hospital at Westmead, Sydney, New South Wales, Australia

⁹Institute of Pediatric Research Citta` della Speranza, Padova, Italy

¹⁰Pathology Unit, Department of Medical and Diagnostic Sciences and Special Therapies, University of Padua, Padua, Italy

Abstract

Soft tissue undifferentiated round cell sarcoma (URCS) occurring in infants is a heterogeneous group of tumors, often lacking known genetic abnormalities. Based on a t(10;17;14) karyotype in a pelvic URCS of a 4-month-old boy showing similar breakpoints with clear cell sarcoma of kidney (CCSK), we have investigated the possibility of shared genetic abnormalities in CCSK and soft tissue URCS. Most CCSK are characterized by *BCOR* exon 16 internal tandem duplications

Corresponding Authors: Cristina R Antonescu, MD, Memorial Sloan Kettering Cancer Center, Pathology Department, 1275 York Ave, New York, NY, 10065, USA; Phone: (212) 639-5905; antonesc@mskcc.org.

Conflicts of interest: none

(ITD), while a smaller subset shows *YWHAE-NUTM2B/E* fusions. Due to overlapping clinicopathologic features, we have also investigated these genetic alterations in the so-called primitive myxoid mesenchymal tumor of infancy (PMMTI). Among the 22 infantile URCS and 7 PMMTI selected, RNA sequencing (RNAseq) was performed in 5 and 2 cases, with frozen tissue, respectively. The remaining cases with archival material were tested for *YWHAE-NUTM2B/E* by FISH or RT-PCR, and *BCOR* ITD by PCR. A control group of 4 CCSK, 14 URCS in older children or adults without known gene fusion, and 20 other sarcomas with similar histomorphology or age at presentation were also tested. A *YWHAE-NUTM2B* fusion was confirmed in the index case by FISH and RT-PCR, while lacking *BCOR* ITD. An identical *YWHAE-NUTM2B* fusion was found in another URCS case of a 5-month-old girl from the back. The remaining cases and control group lacked *YWHAE* gene rearrangements; instead, consistent *BCOR* ITD, similar to CCSK, were found in 15/29 (52%) infantile sarcoma cases (9/22 infantile URCS and 6/7 PMMTI). In the control cohort, *BCOR* ITD was found only in 3 CCSK but not in the other sarcomas. Histologically, URCS with both genotypes and PMMTI shared significant histologic overlap, with uniform small blue round cells with fine chromatin and indistinct nucleoli. A prominent capillary network similar to CCSK, rosette structures and varying degree of myxoid change were occasionally seen. *BCOR* ITD positive tumors occurred preferentially in the somatic soft tissue of trunk, abdomen and head and neck, sparing the extremities. RNAseq showed high *BCOR* mRNA levels in *BCOR* ITD-positive cases, compared to other URCSs. In summary, we report recurrent *BCOR* exon 16 ITD and *YWHAE-NUTM2B* fusions in half of infantile soft tissue URCS and most PMMTI, but not in other pediatric sarcomas. These findings suggest a significant overlap between infantile URCS and CCSK, such as age at presentation, histologic features and genetic signature; thus raising the possibility of a soft tissue counterpart to CCSK.

Keywords

small blue round cell tumor; undifferentiated sarcoma; infantile; *BCOR* ITD; *YWHAE*; clear cell sarcoma kidney; primitive mesenchymal myxoid tumor of infancy

INTRODUCTION

Undifferentiated round cell sarcoma (URCS) is a heterogeneous group of tumors composed of tumor cells with monomorphic round nuclei and scant cytoplasm, that usually lacks a known recurrent genetic abnormality and remains unclassified by currently established tumor entities.¹ Based on an index case of a 4-month-old boy with a pelvic round cell sarcoma harboring an identical *YWHAE-NUTM2B* fusion to clear cell sarcoma of kidney (CCSK), we further investigated the possibility of shared genetic abnormalities between CCSK and infantile soft tissue URCS.

CCSK is an aggressive renal sarcoma of young childhood. The classic histologic appearance of CCSK is composed of monotonous round cells with fine to open chromatin, indistinct nucleoli, and delicate chicken-wire capillaries separating the tumor cells into nests. A wide spectrum of morphologies has also been described, including a myxoid background, sclerosing stroma, epithelioid pattern with acinar or rosette-like structures, areas of spindling, storiform growth pattern, rare rhabdoid cytoplasmic inclusions, etc.² Since there

have been no specific confirmatory ancillary tests for CCSK, the diagnosis relies largely on the histomorphology and anatomic presentation in the kidney. Only rare cases of extra-renal CCSK either occurring in other viscera (ileum, ovary)²⁻⁴ or soft tissues^{2,5,6} have been reported. However, recent studies have identified recurrent genetic abnormalities in CCSK, characterized by either internal tandem duplication (ITD) in exon 16 of *BCOR* in the majority of cases or the presence of t(10;17)(q22.3;p13.3) translocation resulting in *YWHAE-NUTM2B/E* fusions in a smaller subset of cases.^{7,8} These two genetic alterations appear to be mutually exclusive.⁹ With these recent advances in the genetic signatures of CCSK, molecular studies can be applied to further investigate the relationship between CCSK and infantile soft tissue URCS.

Another tumor that shares a similar age at presentation and cytomorphology of uniform round to spindle cells is the so-called primitive myxoid mesenchymal tumor of infancy (PMMTI). PMMTI is a soft tissue sarcoma occurring almost exclusively in the trunk, extremities and head and neck of infants, and is histologically composed of sheets of primitive round to spindle cells, a delicate vascular network and a variably myxoid background.¹⁰ The genetic alterations of PMMTI are unknown. Considering the overlapping clinicopathological features, we hypothesized that PMMTI shares similar genetic abnormalities with URCS and CCSK, and thus have investigated the presence of *BCOR* ITD and *YWHAE-NUTM2B/E* fusions in a group of PMMTI.

MATERIALS AND METHODS

Patient selection

The index case was a 4-month-old boy with a pelvic tumor, measuring 8.1 cm, extending to the right retroperitoneum and lumbosacral spinal canal. Computed tomography scan showed that the tumor indented the inferior pole of the right kidney without involving it. The tumor was biopsied and the morphology showed a small blue round cell tumor with round to ovoid nuclei, fine chromatin, indistinct nucleoli, and frequent mitoses (Fig. 1A). A delicate arborizing capillary network was not identified. Conventional cytogenetics found an apparently three-way reciprocal translocation t(10;17;14)(q22.1;p13.3;q24) (Fig. 1B), involving similar regions of chromosome 10 and 17 as reported previously in CCSK.⁸

Aiming for cases of similar age at diagnosis and histology, we selected patients younger than one year of age (infants), diagnosed with a round cell sarcoma, undifferentiated or unclassified sarcoma, or PMMTI, from the consultation archives of three of the senior authors (CTC, RA, CRA). All cases were then tested to exclude known fusion genes, such as *EWSR1*, *FUS*, *CIC*, *BCOR*, *ETV6-NTRK3* by fluorescence in situ hybridization (FISH) or reverse transcription-polymerase chain reaction (RT-PCR). Together with the index case, 29 cases were identified, including 22 URCS and 7 PMMTI (Table 1). Representative hematoxylin and eosin stained slides were reviewed and the following histologic features were recorded: including cytomorphology (round, spindle), mitotic activity, necrosis, vascular network, rosette formation, fibrous septa, and type of stroma (myxoid, sclerotic). Immunohistochemical stains were also reviewed and follow-up information was obtained from the referring pathologists. Two of the PMMTI cases (PMMTI1 and 2) have been previously reported.¹⁰

To further investigate the distribution of these genetic abnormalities among URCS of different age groups and across different tumor entities prevalent in young children, we also included as controls: 14 cases of non-infantile URCS, 2 Ewing sarcomas, 3 *CIC-DUX4* positive round cell sarcomas, 3 *BCOR-CCNB3* positive round cell sarcomas, 1 *BCOR-MAML3* round cell sarcoma,¹¹ 8 rhabdomyosarcomas (3 embryonal rhabdomyosarcoma, 5 spindle cell/sclerosing rhabdomyosarcoma), 2 malignant ectomesenchymomas, and 1 myofibromatosis. Four CCSK were included as positive controls. This study was approved by institutional review board at all participating institutions.

Fluorescence in situ hybridization (FISH)

FISH for *YWHAE* gene break-apart was performed on 4 µm formalin-fixed paraffin-embedded (FFPE) tissue sections. If the result was positive, FISH for *NUTM2B/E* break apart was subsequently performed. Custom probes were made by bacterial artificial chromosomes (BAC) clones (Supplementary Table 1) flanking the *YWHAE* or *NUTM2B/E* gene according to UCSC genome browser (<http://genome.ucsc.edu>) and obtained from BACPAC sources of Children's Hospital of Oakland Research Institute (Oakland, CA; <http://bacpac.chori.org>). The BAC clones were labeled with fluorochromes by nick translation and validated on normal metaphase chromosomes. The slides were deparaffinized, pretreated, and hybridized with denatured probes. After overnight incubation, the slides were then washed, stained with DAPI, mounted with antifade, and examined on a Zeiss fluorescence microscope (Zeiss Axioplan, Oberkochen, Germany) controlled by Isis 5 software (Metasystems). Of the 200 cells counted, > 20% of tumor nuclei with break-apart signals were considered as positive.

RNA sequencing

RNA sequencing (RNAseq) was performed in cases with available fresh frozen tumor tissues, including 7 cases of infantile sarcomas [5 URCS (URCS# 2, 3, 4, 5, 8) and 2 PMMTI (PMMTI# 1, 2)], 2 non-infantile URCS, 1 Ewing sarcoma, 1 *BCOR-MAML3* positive round cell sarcoma, 2 ectomesenchymomas, 1 myofibromatosis, and 5 rhabdomyosarcomas. Total RNA was extracted by RNeasy Plus Mini (Qiagen) from fresh frozen tumor tissues. The mRNA was isolated with oligo(dT) magnetic beads from total RNA (2 µg) and fragmented by incubation at 94°C for 2.5 minutes in fragmentation buffer (Illumina). To reduce the inclusion of artifact chimeric transcripts into the sequencing library, an additional gel size-selection step was introduced before the adapter ligation step. The adaptor ligated library was then enriched by PCR for 15 cycles and purified. The library was sized and quantified using DNA1000 kit (Agilent) on an Agilent 2100 Bioanalyzer according to the manufacturer's instructions. Paired-end RNA sequencing at read lengths of 50 or 51 bp was performed with the HiSeq 2000 (Illumina). All reads were independently aligned with STAR (ver 2.3)¹² and TopHat2 (ver 2.0.14)¹³ against the human reference genome (hg19). Based on the known genetic abnormalities reported in CCSK,^{7,8} the reads were also investigated manually for *YWHAE-NUTM2B/E* fusion and *BCOR* ITD. The mRNA expression of *BCOR* and PEA3 family genes, including *ETV1*, *ETV4* and *ETV5*, were analyzed and compared to other sarcomas.

Reverse transcription-polymerase chain reaction (RT-PCR) for *YWHAE-NUTM2B/E*

RT-PCR was performed to validate the *YWHAE-NUTM2B/E* fusion observed by FISH or RNA sequencing in 2 cases. In addition, 3 cases negative for *YWHAE-NUTM2B/E* fusion by RNAseq were also included as negative control. RNA was extracted from fresh frozen tissues by RNeasy Plus Mini (Qiagen) or from FFPE tissues by Trizol reagent (Invitrogen). The primers were designed with forward primer at exon 5 of *YWHAE* (5'-GCAGAACTGGATACGCTGAGTGAAG-3') and reverse primer at exon 2 of *NUTM2B/E* (5'-GTGTTGTGTGTCACCTCCCCTAC-3' for fresh frozen tissue; 5'-GGCTTCCAACGTCTTTGTCCAG-3' for FFPE tissue), based on the fusion junction reported previously.⁸ As the 2 nearby *NUTM2B* and *NUTM2E* genes share significant homology, we used a consensus primer for RT-PCR screening, the 2 gene transcripts differing by one nucleotide.⁸ RT-PCR was performed using SuperScript III First-Strand Synthesis System (Invitrogen) and Advantage 2 PCR kit (Clontech, Mountain View, CA) at an annealing temperature of 66.0°C for 35 cycles. The PCR products were then analyzed by agarose gel electrophoresis and Sanger sequencing.

PCR for *BCOR* exon 16 ITD

Depending on the material available, genomic PCR or RT-PCR were performed to detect *BCOR* ITD. In one of the CCSK cases, non-neoplastic kidney parenchyma was available and also tested. Genomic DNA was extracted from FFPE tissues by QIAamp DNA FFPE Tissue Kit (Qiagen), except in 5 cases (URCS 1–5), where complementary DNA was synthesized as described above. Primer sequences were designed to target the last exon (exon 16) of *BCOR* (Fwd-1: 5'-GTCCTCCCGCATATTTTCGC-3' or Fwd-2: 5'-GACCTGGAAGCCTTCAACCC-3' and Rev: 5'-CAAGCTGGACCCACCATGTAC-3'). PCR was performed using Advantage 2 PCR kit at annealing temperature of 65.2°C (Fwd-1) or 66.5°C (Fwd-2) for 38 cycles. The PCR products were then analyzed by agarose gel electrophoresis. Amplicons with size larger than wild-type were subsequently sequenced using the Sanger method to confirm the presence of ITD.

Comparison of *BCOR* ITD positive sarcomas gene expression profile with CCSK and *BCOR-CCNB3* positive sarcomas

For the gene expression analysis, all genome-wide RPKM values were quantile normalized and signal intensities were log₂-transformed.¹⁴ The transcriptional profile of the 7 infantile sarcomas (5 URCS, 2 PMMTI) was compared to the gene expression of a large spectrum of sarcomas (n=120) available on the RNAseq platform. A differentially expressed gene list was obtained by using a log₂-Fold-Change threshold of positive 1.3 or negative 5 and a 0.01 false discovery rate (FDR).

We next set out to compare the gene expression signature of *BCOR* ITD and *YWHAE* fusion-positive URCS/PMMTI (described above) with the published transcriptional profile of CCSK and other *BCOR* fusion-positive sarcomas. The previously reported gene expression data from 22 CCSKs (20 *BCOR* ITD and 2 *YWHAE-NUTM2B/E*-positive) and a control group of fetal (n=4) and adult kidney (n=6), available on the Illumina HumanHT-12 V4.0 beadchip platform, GEO (GSE49972), was downloaded¹⁵ and analyzed using a log₂-Fold-Change of negative 5 or positive 1.7 and 0.05 FDR as statistical

thresholds. The differentially expressed gene list obtained was then probe-matched to the RNAseq annotation (hg19) for comparison.

We then obtained the publicly available expression data of 10 *BCOR-CCNB3* fusion-positive round cell sarcomas from GEO (GSE34800)¹⁶ and a control group of normal tissues from GEO (GSE7307) tested on Affymetrix Human Genome U133A Plus 2 platform. For data analysis, Robust Multi-Array Average normalization was performed, including background correlation, quantile normalization, and median polish summary methods.¹⁷ Subsequent analysis was carried out with signal intensities that were log₂-transformed to remove biases based on signal expression values. Statistical t-test and FDR were performed to identify differentially expressed gene list. Differentially expressed gene profile was obtained by the threshold of log₂ negative 5 or positive 2.5 with 0.01 FDR, followed by probe-matched to the RNAseq annotation (hg19).

After the differentially expressed gene list of each tumor entity was defined, we selected a common core gene set, shared by the 3 tumor types by Venn diagram and used it for gene set enrichment analysis (GSEA) and complete-linkage hierarchical clustering for each entity. For GSEA, the gene lists were ranked in the order of signal-to-noise ranking metric between the tumor types (*BCOR* ITD positive URCS/PMMTI, *BCOR* ITD positive CCSK and *BCOR-CCNB3* round cell sarcoma) and the control group available in each platform as mentioned above.

RESULTS

***YWHAE-NUTM2B* fusion is a rare event in infantile URCS**

The clinicopathologic and molecular results of the 29 infantile URCS are summarized in Table 1. Break-apart FISH assay confirmed *YWHAE* and *NUTM2B/E* gene rearrangements in the index case (URCS1) (Fig. 1C). RT-PCR and subsequent direct sequencing showed fusion of exon 5 of *YWHAE* to exon 2 of *NUTM2B* (Fig. 1D). Based on the RNA sequencing data, we identified a second URCS (5 month-old girl, back soft tissue mass) with identical *YWHAE-NUTM2B* fusion (URCS2). This result was further confirmed by RT-PCR and FISH. FISH screening of the remaining infantile URCS/PMMTI and control cases showed no additional cases with break-apart abnormalities in *YWHAE*.

Morphologically, both cases were composed of small round tumor cells with fine to open chromatin, indistinct nucleoli and scant cytoplasm. A prominent branching vascular network reminiscent of CCSK was present in URCS2 (Fig. 2A). There was no obvious myxoid stroma or rosette formation. Lymphovascular invasion was noted in URCS2. CD99 immunostains were negative in both cases. The index case developed brain metastasis and died of disease 3 months after diagnosis. URCS2 was a recent case with no follow-up information available to date.

***BCOR* ITD is the most frequent genetic event in infantile soft tissue URCS**

In the remaining 4 URCS with RNA sequencing results, all of them were found to have *BCOR* exon 16 ITD, which was subsequently confirmed by RT-PCR or genomic PCR. Furthermore, 5 additional URCS cases were positive for *BCOR* ITD by genomic PCR from

FFPE tissues. Thus a total of 9 infantile URCS out of 22 tested (41%) were positive for *BCOR* ITD (Table 1, Fig. 3A). The duplicated sequence from the *BCOR* exon 16 varied in size (66–99 bp) and genomic position; 8 of the positive cases encompassing 4 different variants (Fig. 3A), while the ITD variant was undetermined in one case.

Among the patients with *BCOR*-ITD positive tumors, there were 6 males and 3 females (male-to-female ratio, 2:1), with an age at presentation ranging from 8 days to 11 months old. The tumors occurred in the somatic soft tissue of trunk (5), pelvis/retroperitoneum (2), and head and neck (2). Morphologically, most cases were composed of sheets or lobules of monotonous small round cells with fine chromatin. The characteristic delicate arborizing capillary network was observed diffusely in 3 cases and focally in one (Fig. 2B). Two cases had cellular fibrous septa as seen in CCSK (Fig. 2C). Variable degree of myxoid stromal change was noted in 5 cases, including 1 with extensive cystic change (Fig. 2D). Two cases showed well-formed rosette structures (Fig. 2E). Most cases showed scant cytoplasm, but clear or vacuolated cytoplasm was noted in 3 cases (diffuse in 2, focal in one)(Fig. 2F), and appeared to coalesce into microcystic spaces in one case. Focal multinucleated giant cells with smudged nuclei were seen in one case (URCS4, 2nd recurrence). Most of the cases were mitotically active (>4/10 HPFs in 66% cases), except for cases with extensive myxoid change which had lower mitotic counts. Some showed abundant karyorrhexis. Lymphovascular invasion was noted in one case. CD99 membranous immunostaining was positive in 3 out of 6 cases (2 diffuse, 1 focal). There was no obvious association between ITD variants and tumor location, gender, degree of myxoid change, or the presence of a delicate vascular pattern. Both cases with prominent rosette formation had the same ITD subtype. Follow-up information was available in 3 patients: one experienced 4 loco-regional recurrences and succumbed to the disease 26 months after diagnosis; one had a local recurrence 4 months after diagnosis; the third has shown no evidence of disease (NED) 41 months after diagnosis.

PMMTI share similar *BCOR* ITD with soft tissue infantile URCS and CCSK

From the 7 PMMTI examined, all except one case (86%) were found to be positive for *BCOR* ITD, 2 by RNA sequencing and 4 by genomic PCR. There were 4 *BCOR* ITD variants identified (63–120 bp, Fig. 3A), including one identical to URCS, while the ITD variant could not be determined in one case.

The 6 PMMTI harboring *BCOR* ITD affected patients between 2 to 10 months old, with equal gender distribution. The location of the tumors included soft tissue of trunk (3), abdomen/retroperitoneum (2) and larynx (1). Tumor sizes ranged from 2.5 cm to 5.5 cm in the three cases (PMMTI1, 2, 6) with available information. There was significant morphologic overlap with CCSK and URCS, but the PMMTI cases showed more prominent myxoid stroma. The tumor cells were predominantly round to ovoid (Fig. 4A), less frequently stellate (2 cases, Fig. 4B) and rarely spindled (one case, Fig. 4C). Chicken-wire branching vasculature was also present in 5 cases, being diffuse in 4 and focal in one (Fig. 4D). One case also showed the presence of cellular fibrous septa (Fig. 4E), similar to that seen in CCSK and some cases of infantile URCS. Vacuolated cytoplasm or rhabdoid morphology was observed in 2 cases each (Fig. 4F-G). One case had lymphovascular

invasion. CD99 staining was not performed in these cases and no additional material was available for further immunohistochemical stains. One patient died of disease 5 years after diagnosis, while the other 2 patients are alive with disease after a short follow-up available (5 and 6 months, respectively, see Table 1).

The only PMMTI case negative for *BCOR* ITD occurred in a 21 month-old boy, who developed a gradually enlarging thigh mass since he was 17 months old. Histologically, it was composed of ovoid to stellate tumor cells in a myxoid background accompanied by a delicate vasculature throughout, almost indistinguishable from other PMMTIs, except that the chromatin pattern was slightly more clumped (Fig. 4H).

No *YWHAE-NUTM2B/E* fusions or *BCOR* ITDs are identified in other infantile or non-infantile sarcomas—None of the other tumors included in the control group were found to share these genetic abnormalities, as investigated by FISH for *YWHAE* rearrangement, PCR for *BCOR* ITD and/or RNA sequencing. As expected, 3 out of 4 CCSKs were positive for *BCOR* ITD, but none showed *YWHAE* gene rearrangement. The non-neoplastic renal parenchyma of one CCSK case was negative for *BCOR* ITD in contrast to the adjacent tumor, excluding a constitutional genetic change. The *BCOR* ITD variants were different from each other in the 3 CCSK cases, including one previously unreported variant (Fig. 3A).^{7,9,18,19} Two of the *BCOR* ITD-positive CCSKs were diagnosed in adult patients, both 29 year-old male patients, and the third being a 5-year-old boy.

Upregulation of *BCOR* mRNA is a common feature of URCS/PMMTI and CCSK with either *BCOR* ITD, *YWHAE-NUTM2B*, or *BCOR*-related-fusions

By RNA sequencing, all *BCOR* ITD-positive tumors (4 URCS, 2 PMMTI) showed a very high level of *BCOR* mRNA expression (Fig. 5B). The high *BCOR* expression was not restricted to the last exon, where the ITD occurred, but spanned throughout the entire transcript (data not shown). An intermediate level of *BCOR* overexpression was also noted in the *YWHAE-NUTM2B* positive URCS and in the *BCOR-MAML3* positive round cell sarcoma, but not in other sarcomas available on our RNAseq platform (Fig. 5B). Furthermore, *BCOR* up-regulation was also identified in the CCSKs with either *BCOR* ITD or *YWHAE* fusion and in *BCOR-CCNB3* positive round cell sarcoma from the published data (Fig. 5B). In contrast to *CIC-DUX4* positive sarcomas, *ETV1*, *ETV4* and *ETV5* mRNA expressions were not up-regulated in *BCOR*-ITD URCS/PMMTI (data not shown).

The gene signature of *BCOR* ITD positive URCS/PMMTI shows significant overlap with CCSK and *BCOR-CCNB3* positive sarcoma

By unsupervised clustering, the URCS and PMMTI with *BCOR* ITD grouped together in a distinct cluster from other sarcomas (Fig. 3B). The *YWHAE-NUTM2B* fusion positive URCS also clustered together with the *BCOR* ITD URCS (Fig. 3B). A gene list of 404 differentially expressed genes was obtained as the *BCOR* ITD gene signature of URCS and PMMTI based on our RNA sequencing data. From the publicly available CCSK dataset, we obtained a 359 differentially expressed gene list compared to normal kidney. Comparing the gene signature of CCSK to that of *BCOR* ITD-positive URCS/PMMTI, we identified 119 (33%) overlapping genes (Fig. 5A). Among them, 44 genes were also upregulated in the

BCOR-CCNB3 fused round cell sarcoma (Fig. 5A). The GSEA algorithm showed significant enrichment (FDR < 0.25) of this 44 gene list across the 3 tumor datasets obtained from different platforms (Fig. 5A). Hierarchical clustering using the same 44 gene list showed a distinct cluster of *BCOR* ITD-positive URCS/PMMTI from other sarcomas. In addition, the *YWHAE-NUTM2B* and *BCOR-MAML3* fusion-positive URCS also grouped with *BCOR* ITD-positive URCS. Similarly, in the CCSK cohort, the 2 *YWHAE-NUTM2B/E*-positive cases grouped together with *BCOR* ITD-positive tumors and separate from the non-neoplastic kidney samples. Furthermore, using this common gene list, the *BCOR-CCNB3* positive sarcomas grouped together but separate from the Ewing sarcomas and normal tissues. Expression levels of representative upregulated genes from the 44 gene list, including *BCOR*, *ZIC2*, *PITX1*, *LHX2*, *SATB2*, and *KDM2B*, are shown in Figure 5B.

Upon review, there was also a morphologic overlap noted among *BCOR* ITD-positive URCS/PMMTI, CCSK, and URCS with *BCOR-MAML3* and *BCOR-CCNB3* fusion (Fig. 6). The tumor nuclei showed homogeneous fine chromatin pattern, lacking prominent nucleoli. The delicate vascular network was also observed in our control cases of CCSK (Fig. 6A) and *BCOR-MAML3* URCS (Fig. 6B). Some areas of myxoid stromal change and more oval to short spindle tumor cells were also seen in *BCOR-CCNB3* sarcoma.

DISCUSSION

Infantile/congenital sarcomas with a round cell phenotype are uncommon and often diagnostically challenging. In contrast to the spindle cell sarcomas that frequently occur in this age group, such as *ETV6-NTRK3* fusion-positive infantile fibrosarcoma²⁰ and less commonly congenital spindle cell rhabdomyosarcoma with *VGLL2*-related fusions,²¹ most of the well-established round cell sarcoma entities, such as Ewing sarcoma, desmoplastic round cell sarcoma, or sarcomas with *CIC-DUX4* or *BCOR-CCNB3* fusions rarely occur in infants.^{16,22–28} In fact, in our database of 31 infantile round cell sarcomas occurring in soft tissue, only 2 (6.5%) cases had known gene fusions (one *EWSR1-ERG*, the other *EWSR1-ETV4*). With relatively non-specific histomorphology and largely unknown genetic abnormalities, many of these cases thus fall into the category of undifferentiated round cell sarcoma.

Interestingly, CCSK is also a sarcoma with round cell phenotype, which almost always occurs in the kidneys of young children, with an age range at diagnosis between 2 months and 14 years, with a mean of 36 months and median of 30 months.² The genetic hallmark of CCSK was characterized recently as either harboring *BCOR*-ITD in most cases⁷ or a *YWHAE-NUTM2B/E* fusion in 12% of cases,⁸ molecular abnormalities which appear to be mutually exclusive.⁹ Rare cases of extrarenal CCSK have been reported, including 3 infants with tumors involving soft tissue of the neck,⁵ terminal ileum⁴ and ovary,^{2,3} respectively, and 2 teenagers (13 and 11 years old) with tumors involving pelvic cavity^{2,6} and retroperitoneum,² respectively. To our knowledge, only the neck mass of a 3-week-old boy, which was histologically similar to CCSK, was reported to harbor a *YWHAE-NUTM2B/E* fusion,⁵ while the fusion status of other extra-renal CCSK cases are unknown. No *BCOR* ITD data has been reported to date in extra-renal CCSK or soft tissue sarcomas.

In this study, we identified a *YWHAE-NUTM2B* fusion in 2 (9%) and *BCOR* ITD in 9 (41%) cases of 22 infantile URCS of soft tissue studied. There were 7 males and 4 females, with an age range of 8 days to 11 months. The tumors occurred preferentially in the soft tissue of trunk, pelvis/retroperitoneum, and head and neck, sparing the extremities. Our results are in keeping with prior observations that the presence of *BCOR* ITD and *YWHAE-NUTM2B/E* fusions are mutually exclusive molecular events in URCS as they are in CCSK.⁹ URCS with these 2 genetic abnormalities share similar histologic features as well as significant overlap with the wide morphologic spectrum of CCSK.² As seen in the classic pattern of CCSK, many of these soft tissue URCS were composed of a proliferation of uniform round cells with open chromatin and a delicate arborizing capillary network. In addition, the less common patterns described in CCSK, such as myxoid pattern or epithelioid pattern with acinar or rosette-like structures,² were also seen in the *BCOR-ITD/YWHAE* positive soft tissue URCS. In the pathologic studies prior to the identification of these genetic abnormalities, the classic histologic pattern was noted in more than 90% of renal CCSKs at least focally.² In the present soft tissue cohort of infantile URCS, the 'classic CCSK pattern' was seen in 5/11 (45%) cases harboring either a *YWHAE* rearrangement or *BCOR* ITD. No distinct morphologic features were noted in the infantile soft tissue URCS lacking both genetic abnormalities.

Interestingly, *BCOR* ITD were also identified in the majority of cases diagnosed as PMMTI (6/7, 86%). Initially classified among infantile fibrosarcomas due to overlapping histology and demographics, PMMTI was subsequently recognized as a distinct entity of possible fibroblastic-myofibroblastic derivation based on its lack of *ETV6-NTRK3* genetic abnormality, distinctive primitive cells, myxoid background, and a more locally aggressive clinical behavior compared to infantile fibrosarcoma.¹⁰ The largest series of PMMTI reported to date encompassed 6 cases, with a narrow age range of 0–2 months old and a wide anatomic distribution, including trunk, extremity, and head and neck.¹⁰ All except one of their patients with available clinical information had local recurrence or persistent disease, but most were still alive at the last follow-up. Histologically, the tumors were described as having a myxoid background, delicate vascular network, and primitive spindle, polygonal to round tumor cells. Focal short spindle cell fascicles may also be seen. Aside from the soft tissue location, PMMTI shares some clinicopathologic overlap with CCSK. In this study, we included 2 cases (case 1 and 4) from the initial PMMTI cohort¹⁰ and 4 additional cases diagnosed as PMMTI. Similar to URCS cases, *BCOR* ITD was only identified in PMMTI occurring in patients under the age of one (2–10 month-old); the tumors presenting in the soft tissue of trunk, abdominal cavity/ retroperitoneum and rarely head and neck. Based on these overlapping clinicopathologic features, we propose that PMMTI and a subset of infantile URCS might represent the soft tissue counterpart of CCSK.

Although our study included a large cohort of soft tissue URCS, spanning a wide age range (infants, older children, adolescents, adults), the two genetic abnormalities: *YWHAE-NUTM2B* fusion and *BCOR* ITD were found exclusively in infants. None of the older patients with URCS studied (range 3–29 years) had *BCOR* ITD or *YWHAE* rearrangements. Moreover, the only case of extra-renal CCSK with a reported *YWHAE-NUTM2B/E* fusion occurred also in a 3-week-old infant.⁵ This finding is intriguing, since renal CCSK harboring similar genetic abnormalities show a broader age range at diagnosis: 0–9 years for the

BCOR ITD-positive cases^{7,9,18,19} and 0.5–6 years in *YWHAE*-rearranged CCSK.^{8,29} Of interest, among the CCSK positive control cases included in our series, 2 of the 3 CCSKs with *BCOR* ITD were both 29-year-old male patients, which appear to be the oldest CCSK patients with this genetic abnormality reported to date.

Similar to CCSK, the duplicated *BCOR* sequences were all in-frame and consistently located in the last exon of *BCOR*, although they were variable in the number of nucleotides and the genomic positions. Comparing the spectrum of *BCOR* ITD variants seen in soft tissue URCS/PMMTI, there were a number of them similar to the ones described in renal CCSK,^{7,9,18,19} but also several novel ITD variants, with a wider size range (63–120 bp). The common duplicated region of 13 amino acids previously described in CCSK was also present in all of our URCS *BCOR* ITD variants.⁷

BCOR (BCL-6 interacting corepressor) was first described to interact with BCL-6 POZ domain via its BCOR BCL6-binding domain and potentiate the transcriptional repression of BCL-6.^{30,31} *BCOR* is also part of a subtype of polycomb repressive complex 1 (PRC1), together with PCGF1, RING1B, and KDM2B. In this complex, the PUF (PCGF Ub-like fold discriminator) domain of BCOR, located at the C terminus, binds to PCGF1 (polycomb-group RING finger homologue 1)(Fig. 3A).^{32,33} This BCOR complex, categorized as a non-canonical PRC1 complex, regulates gene transcription through an epigenetic silencing mechanism. It is recruited to nonmethylated CpG islands and catalyzes demethylation of H3K36me2 and monoubiquitylation of H2AK119.³⁴ It has been shown to play a role in embryonic stem cell differentiation and the regulation of mesenchymal stem cell function.^{35,36}

Genetic alterations in *BCOR* have been reported in several human diseases. Germline *BCOR* loss of function mutations (truncation, frameshift) result in X-linked oculofaciocardiodental (OFCD) syndromes, presenting with congenital cataracts, dysmorphic facies, cardiac abnormalities, radiculomegaly and associated with male lethality.³⁷ In cancer, somatic mutations of *BCOR* have been detected in a small subset of acute myeloid leukemia, myelodysplastic syndrome and chronic myelomonocytic leukemia.³⁴ Chromosomal rearrangements involving *BCOR* have also been found in round cell sarcomas (*BCOR-CCNB3*; *BCOR-MAML3*),^{11,16} endometrial stromal sarcoma and ossifying fibromyxoid tumor (*ZC3H7B-BCOR*),^{38,39} and acute myeloid leukemia (*BCOR-RARα*).⁴⁰ In CCSK and infantile round cell sarcoma with *BCOR* ITD, the ITD sequences located at the C-terminal may affect the PUF domain conformation of the BCOR protein. The additional stretch of amino acids (ITD) in the PUF domain might interfere with PCGF1 binding and thus could affect the PRC1-related epigenetic modifications; although the exact mechanism remains to be investigated.

A high *BCOR* mRNA expression, spanning the entire transcript rather than restricted to the exon 16 ITD region, was identified in all *BCOR* ITD positive URCS and PMMTI, as previously documented in CCSK.^{7,18,19} Furthermore, *BCOR* up-regulation was also detected in our *YWHAE-NUTM2B* fusion positive URCS, similar to the 2 previously reported fusion-positive CCSK cases.⁹ These results suggest that despite the 2 different genetic abnormalities seen in URCS, PMMTI and CCSK spectrum, a common core of

BCOR mRNA overexpression is present, which may trigger a similar downstream pathway. Moreover, transcriptional *BCOR* upregulation was also found in the *BCOR-MAML3* and *BCOR-CCNB3* round cell sarcomas.^{11,16} These findings suggest different mechanisms of *BCOR* overexpression, either through conventional gene fusions or ITD, and may emerge as a critical molecular event in these URCS. In addition to *BCOR* upregulation, URCS/PMMTI and CCSK further shared a significant transcriptional signature resulting in a tight clustering pattern of URCS/PMMTI and CCSK, respectively, from their appropriate control groups. Of interest, *BCOR-CCNB3* round cell sarcoma also shared a transcriptional profile similar to *BCOR* ITD neoplasia. In light of these findings, we observed in retrospect certain histologic overlap between our *BCOR* ITD-positive soft tissue URCS and other URCS with *BCOR*-related gene fusions. In contrast to classic Ewing sarcoma and *CIC-DUX4* fusion positive URCS, *BCOR-CCNB3*^{27,41} and *BCOR-MAML3*¹¹ fusion positive tumors more often display an oval to spindle cell phenotype, with myxoid areas, thus showing overlapping morphologic features with *BCOR* ITD infantile URCS and renal CCSK tumors. Furthermore, the limited data available on patients with *BCOR-CCNB3* tumors suggests that the clinical behavior might be less aggressive than other Ewing sarcoma family of tumors.²⁷ In contrast to the *CIC-DUX4* positive sarcomas, *BCOR* ITD positive and *YWHAE* rearranged URCS did not show upregulation of the PEA3 family of transcription factors, including *ETV1*, *ETV4*, and *ETV5*.⁴² However, further investigations including functional studies are required to assess more definitively the pathogenetic link between these pathologic entities sharing *BCOR* mRNA overexpression.

In conclusion, we report 17 cases of infantile URCS/PMMTI with identical genetic abnormalities to CCSK, including either ITD in the last exon of *BCOR* or *YWHAE-NUTM2B* fusion. Moreover, our results show a significant demographic and morphologic overlap between this subset of URCS in infants, PMMTI and CCSK, suggesting a single disease entity affecting this age group. Our results also raise the possibility of further genetic links with other *BCOR*-fusion related sarcomas (i.e. *BCOR-MAML3* and *BCOR-CCNB3*). Our data also suggests that the detection of *BCOR*-ITD by PCR or *YWHAE* gene rearrangement by FISH can be used in clinical practice for confirming this diagnosis in challenging cases of soft tissue tumors in infants. Further investigations are needed to evaluate the biologic behavior of these patients, as our study had very limited clinical follow-up. Moreover, larger studies are also required to investigate the appropriate therapeutic modalities for this genetically distinct group of tumors, and if they could benefit from the current intensive treatment protocol which has improved the prognosis for CCSK.^{2,43,44}

Supplementary Material

Refer to Web version on PubMed Central for supplementary material.

Acknowledgments

Supported in part by: P50 CA140146-01 (CRA); P30-CA008748 (CRA); Kristen Ann Carr Foundation (CRA), Cycle for Survival (CRA).

References

1. Fletcher, C.; Bridge, JA.; Hogendoorn, PC., et al. WHO Classification of Tumours of Soft Tissue and Bone. IARC; Lyon: 2013.
2. Argani P, Perlman EJ, Breslow NE, et al. Clear cell sarcoma of the kidney: a review of 351 cases from the National Wilms Tumor Study Group Pathology Center. *Am J Surg Pathol.* 2000; 24:4–18. [PubMed: 10632483]
3. Finn LS, Patterson K. Ovarian sarcoma with pathologic features of clear cell sarcoma of the kidney. *Pediatr Dev Pathol.* 2000; 3:487–491. [PubMed: 10890934]
4. Kataoka Y, Shimada H, Sugimoto T, et al. Congenital sarcoma in the terminal ileum histologically resembling clear cell sarcoma of the kidney: a case report with an immunohistochemical study. *Hum Pathol.* 1993; 24:1026–1030. [PubMed: 7504650]
5. Fehr A, Hansson MC, Kindblom LG, et al. YWHAE-FAM22 gene fusion in clear cell sarcoma of the kidney. *J Pathol.* 2012; 227:e5–7. [PubMed: 22544441]
6. Weeks DA, Malott RL, Zuppan C, et al. Primitive pelvic sarcoma resembling clear cell sarcoma of kidney. *Ultrastruct Pathol.* 1991; 15:403–408. [PubMed: 1755102]
7. Ueno-Yokohata H, Okita H, Nakasato K, et al. Consistent in-frame internal tandem duplications of BCOR characterize clear cell sarcoma of the kidney. *Nat Genet.* 2015; 47:861–863. [PubMed: 26098867]
8. O'Meara E, Stack D, Lee CH, et al. Characterization of the chromosomal translocation t(10;17)(q22;p13) in clear cell sarcoma of kidney. *J Pathol.* 2012; 227:72–80. [PubMed: 22294382]
9. Karlsson J, Valind A, Gisselsson D. BCOR internal tandem duplication and YWHAE-NUTM2B/E fusion are mutually exclusive events in clear cell sarcoma of the kidney. *Genes Chromosomes Cancer.* 2016; 55:120–123. [PubMed: 26493387]
10. Alaggio R, Ninfo V, Rosolen A, et al. Primitive myxoid mesenchymal tumor of infancy: a clinicopathologic report of 6 cases. *Am J Surg Pathol.* 2006; 30:388–394. [PubMed: 16538060]
11. Specht K, Zhang L, Sung YS, et al. Novel BCOR-MAML3 and ZC3H7B-BCOR Gene Fusions in undifferentiated small blue round cell sarcomas. *Am J Surg Pathol.* In Press.
12. Dobin A, Davis CA, Schlesinger F, et al. STAR: ultrafast universal RNA-seq aligner. *Bioinformatics.* 2013; 29:15–21. [PubMed: 23104886]
13. Kim D, Pertea G, Trapnell C, et al. TopHat2: accurate alignment of transcriptomes in the presence of insertions, deletions and gene fusions. *Genome Biol.* 2013; 14:R36. [PubMed: 23618408]
14. Mortazavi A, Williams BA, McCue K, et al. Mapping and quantifying mammalian transcriptomes by RNA-Seq. *Nat Methods.* 2008; 5:621–628. [PubMed: 18516045]
15. Karlsson J, Holmquist Mengelbier L, Ciornei CD, et al. Clear cell sarcoma of the kidney demonstrates an embryonic signature indicative of a primitive nephrogenic origin. *Genes Chromosomes Cancer.* 2014; 53:381–391. [PubMed: 24488803]
16. Pierron G, Tirode F, Lucchesi C, et al. A new subtype of bone sarcoma defined by BCOR-CCNB3 gene fusion. *Nat Genet.* 2012; 44:461–466. [PubMed: 22387997]
17. Richter GH, Plehm S, Fasan A, et al. EZH2 is a mediator of EWS/FLI1 driven tumor growth and metastasis blocking endothelial and neuro-ectodermal differentiation. *Proc Natl Acad Sci U S A.* 2009; 106:5324–5329. [PubMed: 19289832]
18. Astolfi A, Melchionda F, Perotti D, et al. Whole transcriptome sequencing identifies BCOR internal tandem duplication as a common feature of clear cell sarcoma of the kidney. *Oncotarget.* 2015; 6:40934–40939. [PubMed: 26516930]
19. Roy A, Kumar V, Zorman B, et al. Recurrent internal tandem duplications of BCOR in clear cell sarcoma of the kidney. *Nat Commun.* 2015; 6:8891. [PubMed: 26573325]
20. Minard-Colin V, Orbach D, Martelli H, et al. Soft tissue tumors in neonates. *Arch Pediatr.* 2009; 16:1039–1048. [PubMed: 19398311]
21. Alaggio R, Zhang L, Sung YS, et al. A Molecular Study of Pediatric Spindle and Sclerosing Rhabdomyosarcoma: Identification of Novel and Recurrent VGLL2-related Fusions in Infantile Cases. *Am J Surg Pathol.* 2016; 40:224–235. [PubMed: 26501226]

22. Maygarden SJ, Askin FB, Siegal GP, et al. Ewing sarcoma of bone in infants and toddlers. A clinicopathologic report from the Intergroup Ewing's Study. *Cancer*. 1993; 71:2109–2118. [PubMed: 8443760]
23. Jinkala SR, Basu D, Mathath D, et al. A rare case of congenital Ewing sarcoma/PNET of the scapula. *J Pediatr Hematol Oncol*. 2014; 36:e134–135. [PubMed: 24072238]
24. Salgado C, Neff T, Frazier L, et al. An unusual case of congenital primitive neuroectodermal tumor with ocular metastasis. *J Pediatr Hematol Oncol*. 2012; 34:e69–71. [PubMed: 22052164]
25. Choi EY, Thomas DG, McHugh JB, et al. Undifferentiated small round cell sarcoma with t(4;19)(q35;q13.1) CIC-DUX4 fusion: a novel highly aggressive soft tissue tumor with distinctive histopathology. *Am J Surg Pathol*. 2013; 37:1379–1386. [PubMed: 23887164]
26. Cohen-Gogo S, Cellier C, Coindre JM, et al. Ewing-like sarcomas with BCOR-CCNB3 fusion transcript: a clinical, radiological and pathological retrospective study from the Societe Francaise des Cancers de L'Enfant. *Pediatr Blood Cancer*. 2014; 61:2191–2198. [PubMed: 25176412]
27. Puls F, Niblett A, Marland G, et al. BCOR-CCNB3 (Ewing-like) sarcoma: a clinicopathologic analysis of 10 cases, in comparison with conventional Ewing sarcoma. *Am J Surg Pathol*. 2014; 38:1307–1318. [PubMed: 24805859]
28. Gerald WL, Ladanyi M, de Alava E, et al. Clinical, pathologic, and molecular spectrum of tumors associated with t(11;22)(p13;q12): desmoplastic small round-cell tumor and its variants. *J Clin Oncol*. 1998; 16:3028–3036. [PubMed: 9738572]
29. Karlsson J, Lilljebjorn H, Holmquist Mengelbier L, et al. Activation of human telomerase reverse transcriptase through gene fusion in clear cell sarcoma of the kidney. *Cancer Lett*. 2015; 357:498–501. [PubMed: 25481751]
30. Huynh KD, Fischle W, Verdin E, et al. BCoR, a novel corepressor involved in BCL-6 repression. *Genes Dev*. 2000; 14:1810–1823. [PubMed: 10898795]
31. Ghetu AF, Corcoran CM, Cerchiotti L, et al. Structure of a BCOR corepressor peptide in complex with the BCL6 BTB domain dimer. *Mol Cell*. 2008; 29:384–391. [PubMed: 18280243]
32. Junco SE, Wang R, Gaipa JC, et al. Structure of the polycomb group protein PCGF1 in complex with BCOR reveals basis for binding selectivity of PCGF homologs. *Structure*. 2013; 21:665–671. [PubMed: 23523425]
33. Gearhart MD, Corcoran CM, Wamstad JA, et al. Polycomb group and SCF ubiquitin ligases are found in a novel BCOR complex that is recruited to BCL6 targets. *Mol Cell Biol*. 2006; 26:6880–6889. [PubMed: 16943429]
34. Yamamoto Y, Abe A, Emi N. Clarifying the impact of polycomb complex component disruption in human cancers. *Mol Cancer Res*. 2014; 12:479–484. [PubMed: 24515802]
35. Wamstad JA, Corcoran CM, Keating AM, et al. Role of the transcriptional corepressor Bcor in embryonic stem cell differentiation and early embryonic development. *PLoS One*. 2008; 3:e2814. [PubMed: 18795143]
36. Fan Z, Yamaza T, Lee JS, et al. BCOR regulates mesenchymal stem cell function by epigenetic mechanisms. *Nat Cell Biol*. 2009; 11:1002–1009. [PubMed: 19578371]
37. Ng D, Thakker N, Corcoran CM, et al. Oculofaciocardiodental and Lenz microphthalmia syndromes result from distinct classes of mutations in BCOR. *Nat Genet*. 2004; 36:411–416. [PubMed: 15004558]
38. Antonescu CR, Sung YS, Chen CL, et al. Novel ZC3H7B-BCOR, MEAF6-PHF1, and EPC1-PHF1 fusions in ossifying fibromyxoid tumors--molecular characterization shows genetic overlap with endometrial stromal sarcoma. *Genes Chromosomes Cancer*. 2014; 53:183–193. [PubMed: 24285434]
39. Panagopoulos I, Thorsen J, Gorunova L, et al. Fusion of the ZC3H7B and BCOR genes in endometrial stromal sarcomas carrying an X;22-translocation. *Genes Chromosomes Cancer*. 2013; 52:610–618. [PubMed: 23580382]
40. Yamamoto Y, Tsuzuki S, Tsuzuki M, et al. BCOR as a novel fusion partner of retinoic acid receptor alpha in a t(X;17)(p11;q12) variant of acute promyelocytic leukemia. *Blood*. 2010; 116:4274–4283. [PubMed: 20807888]
41. Peters TL, Kumar V, Polikepahad S, et al. BCOR-CCNB3 fusions are frequent in undifferentiated sarcomas of male children. *Mod Pathol*. 2015; 28:575–586. [PubMed: 25360585]

42. Specht K, Sung YS, Zhang L, et al. Distinct transcriptional signature and immunoprofile of CIC-DUX4 fusion-positive round cell tumors compared to EWSR1-rearranged Ewing sarcomas: further evidence toward distinct pathologic entities. *Genes Chromosomes Cancer*. 2014; 53:622–633. [PubMed: 24723486]
43. Furtwangler R, Gooskens SL, van Tinteren H, et al. Clear cell sarcomas of the kidney registered on International Society of Pediatric Oncology (SIOP) 93-01 and SIOP 2001 protocols: a report of the SIOP Renal Tumour Study Group. *Eur J Cancer*. 2013; 49:3497–3506. [PubMed: 23880476]
44. Gooskens SL, Furtwangler R, Vujanic GM, et al. Clear cell sarcoma of the kidney: a review. *Eur J Cancer*. 2012; 48:2219–2226. [PubMed: 22579455]

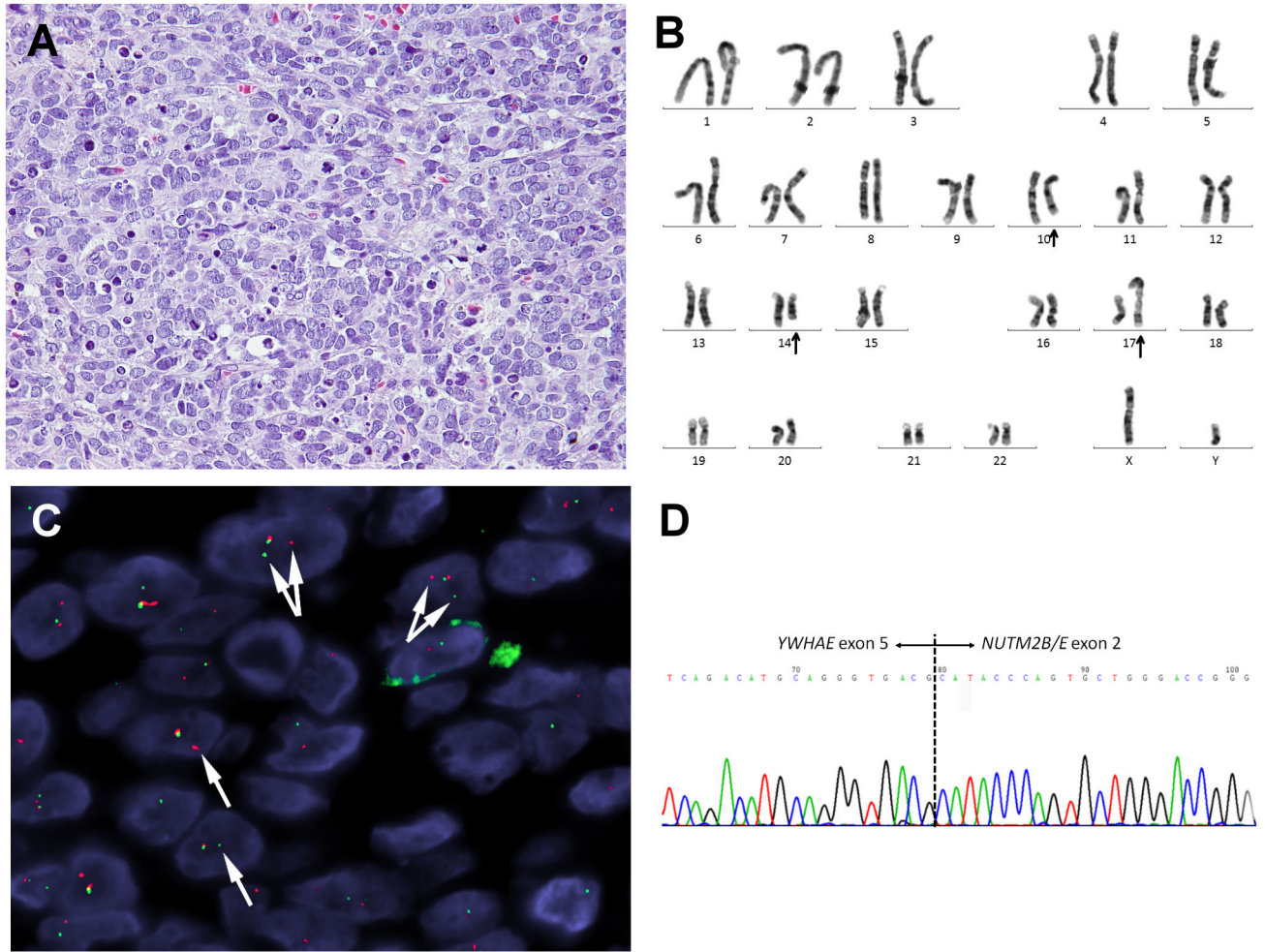


Figure 1. The index URCS case with *YWHAE-NUTM2B* fusion
 Diffuse sheets of monotonous round cells with fine chromatin, indistinct nucleoli, frequent apoptosis and occasional mitoses (A, H&E, 400X). Representative karyotype showing a three-way translocation $t(10;17;14)(q22.1;p13.3;q24)$ indicated by the arrows (B). FISH showing *YWHAE* rearrangement, with break-apart green (telomeric) and red (centromeric) signals (C, white arrows). Sanger sequencing of RT-PCR product demonstrating *YWHAE* exon 5 fused to *NUTM2B* exon 2 (D).

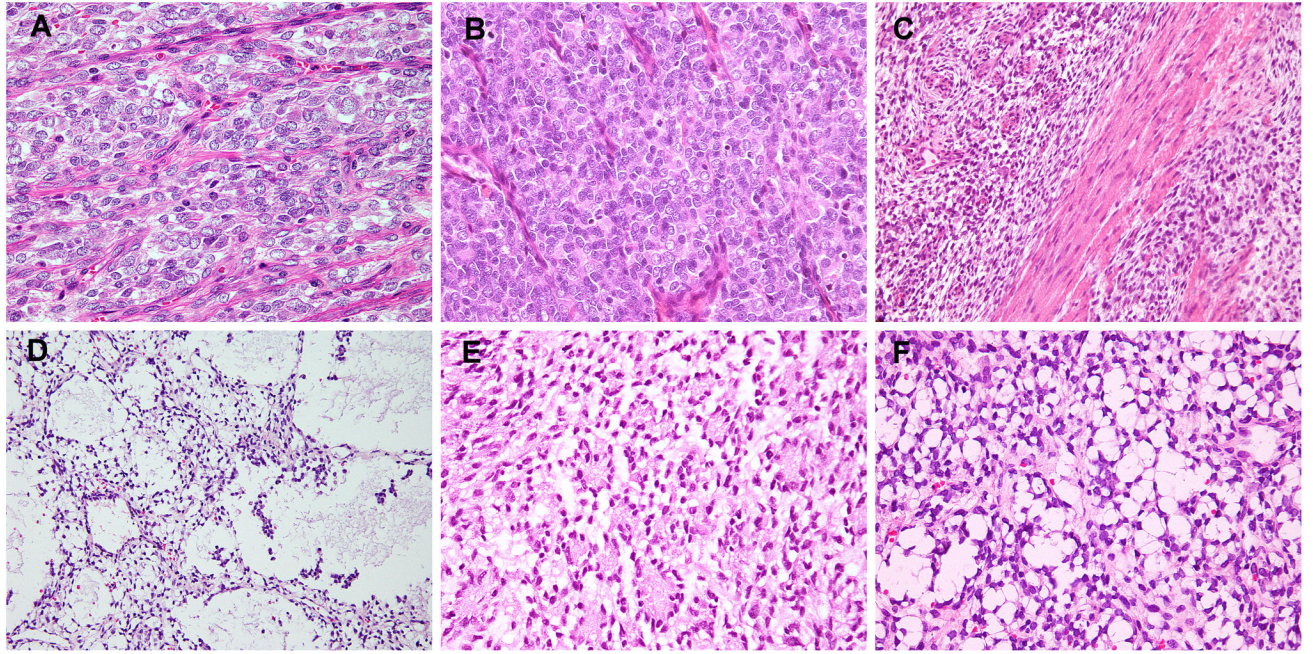


Figure 2. Histology of soft tissue URCS with *YWHAE-NUTM2B* fusion (A) or *BCOR* ITD (B–F) Second case with *YWHAE-NUTM2B* fusion showing delicate arborizing vascular network reminiscent to CCSK (A, URCS2, 200X). *BCOR* ITD URCS showing prominent capillary network (B, URCS3, 100X); cellular fibrous septa (C, URCS3, 200X); uniform round to ovoid tumor cells (B); extensive myxoid stroma and cystic spaces (D, URCS 6, 100X); rosette formation (E, URCS5, 200X) and vacuolated cytoplasm (F, URCS6, 400X).

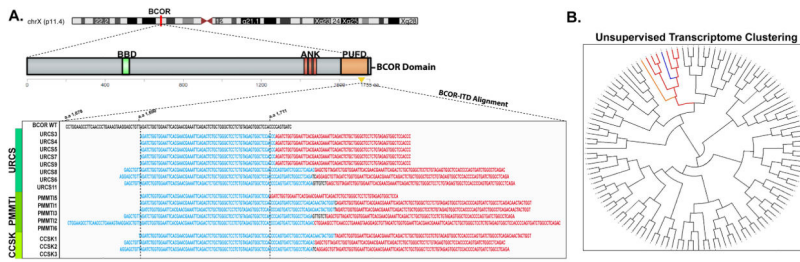


Figure 3. Spectrum of *BCOR* ITD variants in URCS, PMMTI and CCSK samples
 (A) Schematic diagram showing the location of *BCOR* on chromosome Xp11.4, protein domains of *BCOR*, the location of the duplicated sequences on PUF domain, and the ITD subtypes among URCS, PMMTI and CCSK. Compared to wild-type *BCOR*, the original and duplicated sequences are shown in blue and red, respectively. The intervening sequences in black indicate insertions; however, all ITD variants are in-frame. The common region of duplicated sequence is indicated by vertical dot lines. BBD, BCL-6 binding domain; ANK, ankyrin repeat; PUF, PCGF Ub-like fold discriminator. (B) By unsupervised clustering, the URCS/PMMTI with *BCOR* ITD (red), *YWHAE-NUTM2B* fusion (blue) and *BCOR-MAML3* fusion (orange) grouped together in a distinct cluster from other sarcomas available on the RNAseq.

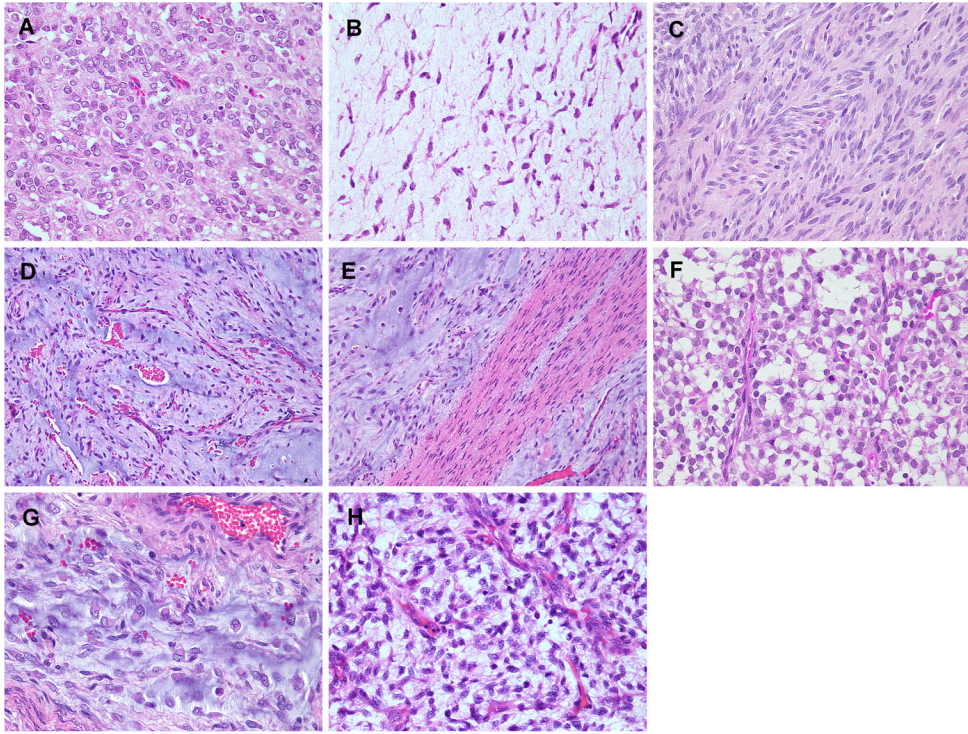


Figure 4. Morphologic spectrum of PMMTI

The PMMTI were associated with a monomorphic cytomorphology, ranging from round (A, PMMTI6, 400X), stellate (B, PMMTI6, 400X) to spindle (C, PMMTI2, 400X). Overlapping histologic features with *BCOR* ITD URCS and CCSK were noted, including rich vascular network (D, PMMTI6, 100X) and cellular fibrous septa (E, PMMTI3, 200X). Other features included occasional cytoplasmic vacuoles (F, PMMTI6, 400X) or rhabdoid cells (G, PMMTI, 400X). The only PMMTI lacking *BCOR* ITD showed ovoid to stellate tumor cells, with slightly clumped chromatin and myxoid stroma (H, PMMTI7, 400X).

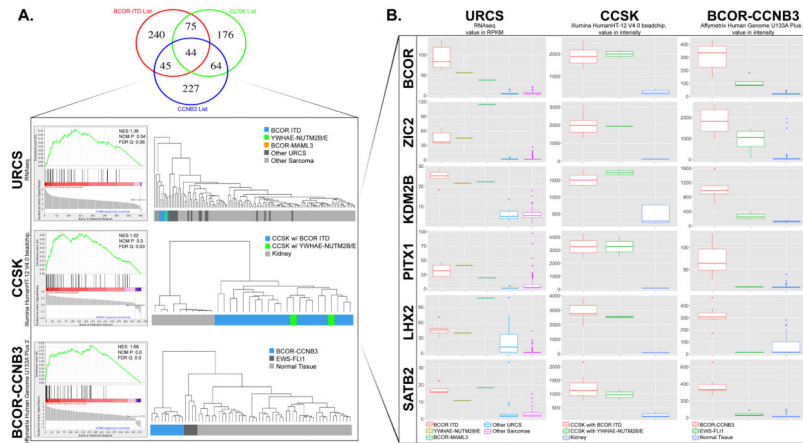


Figure 5. URCS/PMMTI with *BCOR* ITD display overlapping gene signature with CCSK and *BCOR-CCNB3* positive sarcoma

(A) Venn diagram showing overlapping differential gene signature between *BCOR* ITD URCS (RNA-seq data), CCSK (published data, Illumina HumanHT-12 V4.0 beadchip platform)¹⁵, and round cell sarcoma with *BCOR-CCNB3* (published data, Affymetrix Human Genome U133A Plus 2 platform).¹⁶ The GSEA analysis demonstrates enrichment of the 44 genes in common among the 3 tumor categories. Subsequent supervised hierarchical clustering using this 44 gene list revealed that *BCOR* ITD-positive and *YWHAE* fusion-positive tumors grouped together, separate from the control groups. NES, normalized enrichment score; NOM P, nominal p-value; FDR, false discovery rate. (B) Comparative expression of commonly upregulated genes: *BCOR*, *ZIC2*, *KDM2B*, *PITX1*, *LHX2* and *SATB2*, across these 3 tumor entities and individual platforms (URCS with *BCOR* ITD, *YWHAE-NUTM2B*, *BCOR-MAML3* on RNAseq; *BCOR* ITD and *YWHAE-NUTM2B/E* CCSK on Illumina HumanHT-12 V4.0 beadchip platform¹⁵; and round cell sarcoma with *BCOR-CCNB3* on Affymetrix Human Genome U133A Plus 2 platform).¹⁶ ‘Other URCS’ indicates URCS without known genetic alterations.

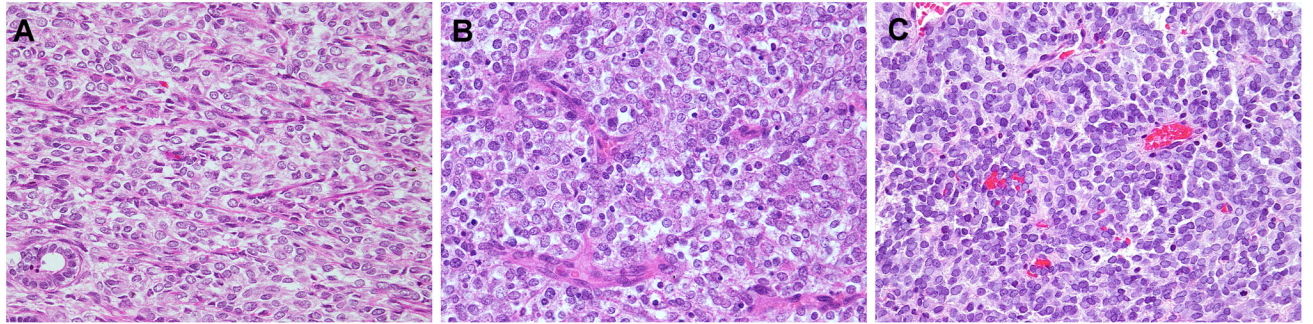


Figure 6. Histologic overlap among CCSK and URCS with *BCOR* ITD and other *BCOR*-related fusions

A similar cytomorphology with fine chromatin and delicate vascular network in CCSK (A, 400X), *BCOR-MAML3* URCS (B, 400X), and *BCOR-CCNB3* URCS (C, 400X).

Table 1
 Clinicopathologic Features and Genetic Abnormalities of Infantile URCS and PMMTI

Case	Age/Sex	Location	Morphology		YWHAE-NUTM2B/E	BCOR ITD	Follow-up
			Rosette	Arb vessels			
URCS1	4 m/M	Pelvic	-	-	+ <i>abc</i>	- <i>c</i>	DR, DOD(3m)
URCS2	5 m/F	Back	-	E	+ <i>bcd</i>	- <i>cd</i>	NA
URCS3	23 d/M	Back	-	E	- <i>cd</i>	+ <i>cd</i>	NA
URCS4	8 d/F	Buttock	+	-	- <i>bcd</i>	+ <i>cd</i>	LR, DOD(26mo)
URCS5	3 m/F	Jaw	+	-	- <i>bcd</i>	+ <i>cd</i>	NED(41mo)
URCS6	3 m/M	RP	-	-	- <i>b</i>	+ <i>e</i>	NA
URCS7	11 m/M	Chest wall	-	-	- <i>b</i>	+ <i>e</i>	NA
URCS8	2 wk/F	Chest wall	-	E	- <i>b</i>	+ <i>de</i>	NA
URCS9	10 d/M	Neck	-	-	- <i>b</i>	+ <i>e</i>	LR(4mo)
URCS10	5 m/M	RP/pelvic	-	Foc	- <i>b</i>	+ <i>e</i>	NA
URCS11	10 m/M	Paravertebral	-	E	- <i>b</i>	+ <i>e</i>	NA
URCS12	1 m/M	Para-anal	-	-	- <i>b</i>	- <i>e</i>	NA
URCS13	10 d/M	Tibia, fibula	-	-	- <i>b</i>	- <i>e</i>	NA
URCS14	6 m/M	Paratesticular	-	-	- <i>b</i>	- <i>e</i>	NA
URCS15	1 y/F	Orbit	-	-	- <i>b</i>	- <i>e</i>	NA
URCS16	1 y/F	Shoulder	-	-	- <i>b</i>	- <i>e</i>	NA
URCS17	1 y/M	Mandible	-	Foc	- <i>b</i>	- <i>e</i>	NA
URCS18	1 y/F	Forearm	-	-	- <i>b</i>	- <i>e</i>	NA
URCS19	1 m/F	Neck	-	-	- <i>b</i>	- <i>e</i>	NA
URCS20	6 m/F	Pelvic	-	-	- <i>b</i>	- <i>e</i>	NA
URCS21	1 y/F	Back	-	Foc	- <i>b</i>	- <i>e</i>	NA
URCS22	9 m/F	Ankle	-	-	- <i>b</i>	- <i>e</i>	NA
PMMTI	2 m/M	Paraspinal	-	Foc	- <i>d</i>	+ <i>de</i>	DR(6m)

Case	Age/Sex	Location	Morphology			YWHAE-NUTM2B/E	BCOR ITD	Follow-up
			Rosette	Arb vessels	Myxoid			
PMMT12	5 m/M	Larynx	-	-	Foc	- _d	+ _{de}	LR, DOD (5y)
PMMT13	9 m/M	Abdominal wall	-	E	E	- _b	+ _e	LR(5m)
PMMT14	6 m/M	RP	-	E	Foc	- _b	+ _e	NA
PMMT15	10 m/F	Abdominal cavity	-	E	Foc	- _b	+ _e	NA
PMMT16	4m/F	Paravertebral	-	E	Foc	- _b	+ _e	NA
PMMT17	1 y/M	Thigh	-	E	Foc	- _b	- _e	NA

Arb, arborizing; m, month; M, male;

^aby conventional cytogenetics;

^bby FISH;

^cby RT-PCR; DR, distant recurrence (metastasis); DOD, dead of disease; F, female; E, extensive;

^dby RNA sequencing; NA, not available; d, day; LR, local recurrence; y, year; Foc, focal; NED, no evidence of disease; RP, retroperitoneum;

^eby genomic polymerase chain reaction; wk, week; AWD, alive with disease.